Chinese Chemical Letters 31 (2020) 1231–1234

Contents lists available at ScienceDirect

Chinese Chemical Letters

journal homepage: www.elsevier.com/locate/cclet

Communication

Supramolecular polymer materials based on pillar[5]arene: Ultrasensitive detection and efficient removal of cyanide

Hong Yao[a,*], Qi Zhou[a], Youming Zhang[a,b], Yinping Hu[a], Xiaotong Kan[a], Yanyan Chen[a], Guanfei Gong[a], Qinpeng Zhang[a], Taibao Wei[a], Qi Lin[a,*]

[a] Key Laboratory of Eco-functional Polymer Materials of the Ministry of Education, Key Laboratory of Eco-environmental Polymer Materials of Gansu Province, College of Chemistry and Chemical Engineering, Northwest Normal University, Lanzhou 730070, China
[b] College of Chemistry and Chemical Engineering, Lanzhou City University, Lanzhou 730070, China

ARTICLE INFO

Article history:
Received 20 August 2019
Received in revised form 11 September 2019
Accepted 23 September 2019
Available online 24 September 2019

Keywords:
Supramolecular polymer gel
Fluorescence detection
Ultrasensitive
Efficient removal
Cyanide

ABSTRACT

An ultrasensitive detection and effective removal material was successfully developed by using a pillar[*n*]arene-based supramolecular polymer gel (**MTP5⊃HB**). The **MTP5⊃HB** can ultrasensitively recognize Cu^{2+} and Fe^{3+}, and the limits of detection (LODs) for Cu^{2+} and Fe^{3+} are 1.55 and 2.68 nmol/L, respectively. Additionally, the *in-situ* generated metallogel **MTP5⊃HB-Cu** can exclusively detect CN^-, and the LOD for CN^- is 1.13 nmol/L. Noticeably, the xerogel of **MTP5⊃HB-Cu** can effectively remove CN^- from aqueous solution with 94.40% removal rate. Test kit based on **MTP5⊃HB-Cu** is also prepared for convenient detection of CN^-.

The extreme toxicity of cyanide (CN^-) in physiological systems, as well as the continuing environmental concern caused by its widespread industrial use, has led to considerable research into development of methods for CN^- detection [1,2]. For example, Mergu *et al.* reported a naphthalimide-benzothiazole conjugate for reaction-based fluorescence detection of CN^- [3]. Shiraishi *et al.* synthesized a coumarin-spiropyran dyad for excellently fluorescent detect CN^- [4]. Although some methods have been developed for the ultrasensitive detection of CN^- [5–7], unfortunately these methods could not remove target ions. While some other methods could efficiently remove CN^- but could not detect CN^- [8]. Therefore, developing novel materials for ultrasensitive detection and efficient removal of CN^- is a charming subject.

Supramolecular polymers are defined as polymeric systems that extend beyond the molecule [9]. Various dynamical and reversible noncovalent interactions promote monomers to assemble into polymeric structures [10,11], which makes them not only possess the merits of traditional covalent polymers but also have some unique performances such as stimuli-response properties [12,13]. Therefore, supramolecular polymers provide a platform for fabricating novel materials with ultrasensitive stimuli responsiveness [14,15]. In addition, pillar[*n*]arenes emerged as new supramolecular host macrocycles was first proposed by Ogoshi in 2008 [16]. The special structure of pillararenes could provide various supramolecular interactions such as H-bonding, π-π stacking, metal coordination, *etc.* [17–19]. These properties endow pillar[*n*]arenes with opportunities for the construction of stimuli responsive supramolecular polymers [20–25].

Aggregation induced emission (AIE), first coined by Tang in 2001 [26], reveals an important photophysical phenomenon that non-emissive luminogens exhibits enhancement of fluorescent emission at aggregate state [27]. In recent years, new type of supramolecular polymer materials with AIE properties has earned much attention in many fields, including biological areas [28], fluorescent sensors [29], optoelectronic systems [30] and stimuli responses materials [31]. Therefore, the research on AIE provide novel approach for the design of ultrasensitive fluorescent stimuli responsive materials [32,33].

Here, a novel pillar[5]arene-based AIE supramolecular polymer gel **MTP5⊃HB** was designed and fabricated referring to the research contents of our previous studies [34]. The **MTP5⊃HB** was constructed by multiple H-bonding and exo-wall π-π stacking interactions between thioacetylhydrazine copillar [5]arene **MTP5** and 2,2′-(1,4-butanediyl)-bis(1*H*-benzimidazole) **HB**. Our strategies are demonstrated as follow. First, the thioacetylhydrazine groups on **MTP5** provides suitable H-bonding interaction sites and metal coordination sites. Then the **HB** supplies electron accepting, π-bridging and metal-ions chelating abilities. Impressively, based on this design, the **MTP5⊃HB** gel is formed and exhibited strong bluish white AIE fluorescence, which can be used to

* Corresponding authors.
E-mail addresses: yhxbz@126.com (H. Yao), linqi2004@126.com (Q. Lin).

https://doi.org/10.1016/j.cclet.2019.09.046
1001-8417/

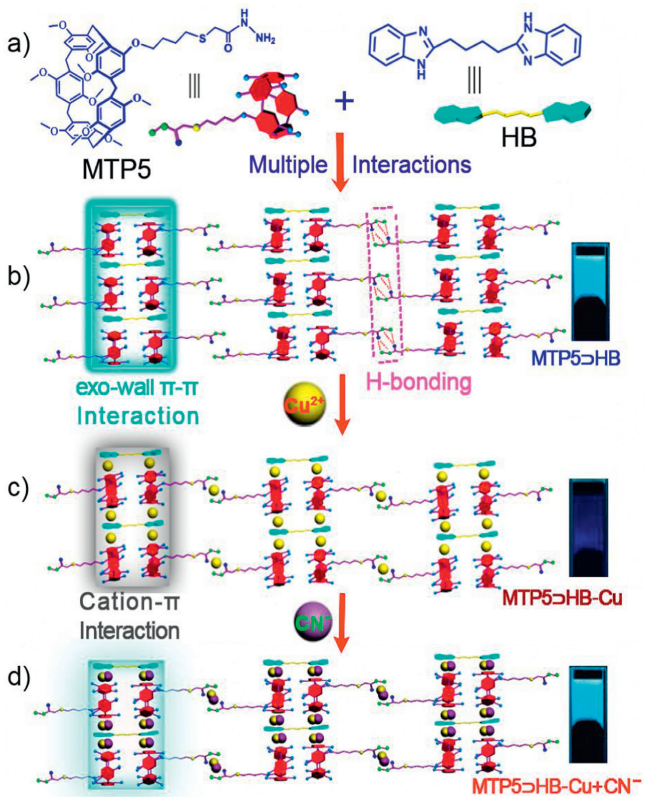

Fig. 1. Schematic illustration for the formation of **MTP5⊃HB** and detection mechanism for ions.

ultrasensitively detect Cu^{2+} and CN^- (Fig. 1). Moreover, the xerogel of *in-situ* generated metallogel **MTP5⊃HB-Cu** has excellent capacity to remove CN^- in water with 94.40% removal rate.

The synthetic route of **MTP5** and **HB** were depicted in Scheme S1 (Supporting information), and they were characterized by ^1H NMR, ^{13}C NMR and HRMS (Figs. S1-S6 in Supporting information). Although **MTP5** could not self-assemble into a supramolecular gel, stable supramolecular polymer gel **MTP5⊃HB** was obtained by mixing it with **HB** in DMSO-H_2O binary solvent containing 35% water (Tables S1 and S2 in Supporting information). As shown in Fig. 2a, the sol of **MTP5⊃HB** had inappreciable

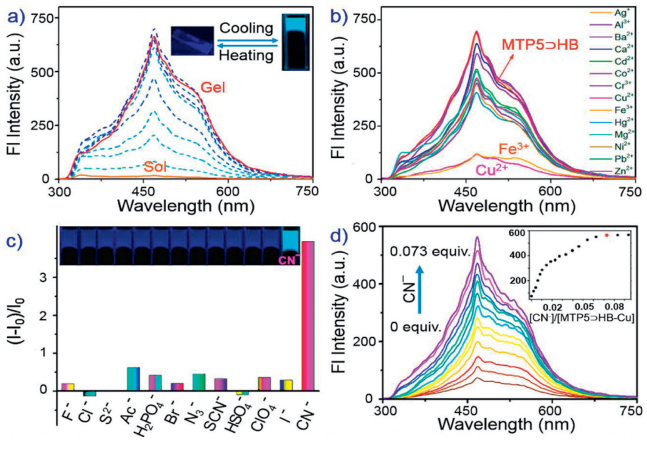

Fig. 2. (a) Temperature-dependent fluorescence spectra of **MTP5⊃HB**. (b) Fluorescence spectra of **MTP5⊃HB** and **MTP5⊃HB-M** (**M** is different cation). (c) Fluorescence enhancement by adding various anions into **MTP5⊃HB-Cu** metallogel. Inset: corresponding photographs under UV lamp irradiation. (d) Fluorescence spectra of **MTP5⊃HB-Cu** with increasing concentration of CN^-. Experiment conditions: wt% = 5%, 35% water fraction in DMSO/H_2O, λ_{ex} = 251 nm.

fluorescence. However, a stable **MTP5⊃HB** gel with a remarkable fluorescence enhancement at 468 nm was generated (wt% = 5%, *i.e.*, 50 mg/mL) when the temperature decreased. Simultaneously, a strong bluish white emission was observed under the irradiation of UV–vis lamp at 365 nm. These results indicated the aggregation-induced emission (AIE) property of **MTP5⊃HB** gel [35].

Series experiments were carried out to further investigated the assembly mechanism of the **MTP5⊃HB**. Firstly, the ^1H NMR titration experiment was performed by gradually adding **HB** into **MTP5**. Upfield shifts in the signals of protons on **HB** were observed, while H_a, H_b and H_c located on **MTP5** shifted slightly to downfield (Fig. S7 in Supporting information), which suggested that π-electron deficient **HB** interacted with electron-rich **MTP5** *via* π-π donor-acceptor interaction [36,37]. Meanwhile, the 2D NOESY NMR spectra exhibited cross peaks at A, B and C (Fig. S8 in Supporting information), which testified that benzimidazole groups on **HB** were close to the aromatic rings on **MTP5**. Then, as shown in the concentration-dependent ^1H NMR spectrum of **MTP5⊃HB** (Fig. 3a), both of H_a, H_b, H_c, H_i, H_h on **MTP5** and H_1, H_2, H_4 on **HB** shifted downfield and became broad with increasing the concentration of **MTP5⊃HB**, indicating the formation of hydrogen-bond between **MTP5** and **HB**. Afterwards, the XRD patterns of xerogel **MTP5⊃HB** showed peaks at 31.47°, 26.75° and 20.21° corresponding to the d-spacing of 2.84 Å, 3.33 Å and 4.39 Å (Fig. 3b), which confirmed that the assembly process of **MTP5⊃HB** was promoted by the combination of H-bonding, exo-wall π-π stacking and intercolumnar stacking interactions [37–39]. In addition, there was a peak at *m/z* 1187.5522 in the HRMS spectrum of **MTP5⊃HB** (Fig. S9 in Supporting information), which could be assigned for [**MTP5** + **HB** + H]$^+$. This result indicated that **MTP5** combined with **HB** in 1:1 stoichiometric ratio. Finally, the SEM morphological features of xerogel **MTP5⊃HB** showed a regular overlapping laminar morphology (Fig. 4a), which supported the formation of a 3D network structure of **MTP5⊃HB**.

The fluorescence detection property of **MTP5⊃HB** for cations was studied by diffusing various cations (including Fe^{3+}, Zn^{2+}, Mg^{2+}, Co^{2+}, Zn^{2+}, Hg^{2+}, Ag^+, Ca^{2+}, Cu^{2+}, Ni^{2+}, Cr^{3+}, Pb^{2+}, Cd^{2+} and Ba^{2+}, c = 0.1 mol/L) into **MTP5⊃HB**, only Cu^{2+} and Fe^{3+} ions quenched the fluorescence emission (Fig. 2b). Moreover, the detection limits (LODs) of **MTP5⊃HB** toward Cu^{2+} and Fe^{3+} were determined by fluorescence titration as 1.55 nmol/L and 2.68 nmol/L, respectively (Figs. S10 and S11 in Supporting information), which indicated the sensitivity of **MTP5⊃HB** were much higher than other reported sensors (Table S3 in Supporting information). After that, the anions recognition performance of *in-situ* generated metallogel **MTP5⊃HB-Cu** was investigated by adding different anions such as F^-, Cl^-, S^{2-}, Ac^-, $H_2PO_4^-$, Br^-, N_3^-, SCN^-, HSO_4^-, ClO_4^-, I^- and CN^- (c = 0.1 mol/L) into these metallogel. As shown in Fig. 2c, **MTP5⊃HB-Cu** could exclusively detect CN^-. Based on the fluorescence titration experiment (Fig. 2d), the LOD of **MTP5⊃HB-Cu** toward CN^- was 1.13 nmol/L (Fig. S12 in Supporting information). Compared with other reported sensors, the **MTP5⊃HB-Cu** possesses higher sensitivity for detecting CN^- (Table 1).

The response mechanisms of supramolecular polymer gel towards Cu^{2+} and CN^- were investigated using FT-IR, XRD and SEM. In the FT-IR spectra (Fig. S15 in Supporting information), the stretching vibration absorption peaks of —NH and —C=O transferred from 3427 cm^{-1} and 1649 cm^{-1} to 3436 cm^{-1} and 1627 cm^{-1}, with the addition of Cu^{2+} into **MTP5⊃HB**. Meanwhile, new shoulder peaks appeared at 1114 cm^{-1} and 2999 cm^{-1}, representing the changes of the stretching vibration absorption peaks of C—S—C and =C—H on aromatic ring, respectively. Moreover, in the XRD spectra (Fig. 3b), the peaks at 3.33 Å and 2.84 Å disappeared, but the peak at 4.39 Å had negligible change. These changes indicated that intercolumnar stacking maintained,

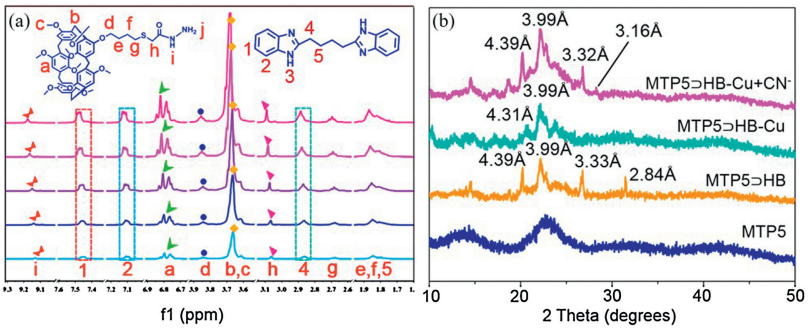

Fig. 3. (a) Partial concentration-dependent ^{1}H NMR spectra (400 MHz, in DMSO-d_6, 298 K) of **MTP5⊃HB**: (bottom to top) 25.0 mg/mL; 50.0 mg/mL; 75.0 mg/mL; 100.0 mg/mL and 125.0 mg/mL (n_{MTP5} : n_{HB} = 1 : 1). (b) Corresponding powder X-ray diffraction patterns.

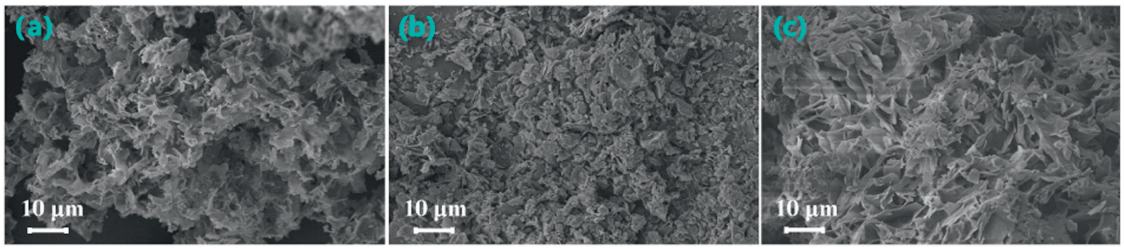

Fig. 4. SEM images of (a) xerogel **MTP5⊃HB**, (b) **MTP5⊃HB-Cu**, (c) **MTP5⊃HB-Cu** + CN^-.

Table 1
Comparison of detection and removal efficiency of **MTP5⊃HB-Cu** for CN^- with other reported sensors.

Detection materials	LOD (nmol/L)	Removal rate (%)	Ref.
Hydrogenated coumarin-spiropyran dyad	1000.00	–	[4]
Graphene quantum dots (GQDs)/gold nanoparticle (AuNPs) conjugate	520.00	–	[1]
Molecular Au(I) cluster	80.00	–	[7]
Ag-core/Au-shell/iridium(III) complex	36.00	–	[2]
Naphthalimide-benzothiazole conjugate	4.50	–	[3]
TiO_2/Fe_2O_3/PAC & TiO_2/Fe_2O_3/zeolite nanophoyocatalysts	–	92.42%, 97.37%	[8]
Magnetic graphene-isolated AuCo nanocrystal	5.00	91.01%	[41]
Pillar[5]arene-based **MTP5⊃HB-Cu**	1.13	94.40%	This work

but H-bonding and exo-wall π-π stacking were destroyed. Additionally, the morphology of xerogel **MTP5⊃HB-Cu** transformed into fragmentary (Fig. 4b). These results showed that the **MTP5⊃HB** combined with Cu^{2+} by coordination interaction with thioacetylhydrazine groups and cation-π interaction.

Moreover, with the addition of CN^- into the **MTP5⊃HB-Cu**, the stretching vibration absorptions of —NH and —C=O shifted to 3429 cm^{-1} and 1643 cm^{-1}, respectively, and the peaks at 2999 cm^{-1} and 1114 cm^{-1} disappeared (Fig. S15). This consequence can be explained by the strong complexation abilities of CN^- with Cu^{2+}, revealing CN^- coordinated with Cu^{2+} in **MTP5⊃HB-Cu**. Moreover, in the XRD, the peaks around 2θ = 26.74° and 28.22° corresponding to the *d*-spacing of 3.32 Å and 3.16 Å appeared again (Fig. 3b), which verified that CN^- coordinated with Cu^{2+} and the exo-wall π-π stacking generated again. In addition, SEM experiment showed the macromorphology changed from fragmentary into regular overlapped layer structure again after adding CN^- into **MTP5⊃HB-Cu** (Fig. 4c). The above results could be ascribed to the competitive coordination mechanism between CN^- and Cu^{2+}.

To explore the application of supramolecular polymer gel **MTP5⊃HB-Cu**, the removal experiment for CN^- were performed. Immersing the xerogel **MTP5⊃HB-Cu** into CN- solution (*c* = 3.40 μmol/L) for three hours, the residual content of CN^- in water was 0.19 μmol/L [40] (Fig. S13 in Supporting information). The removal rate toward CN^- was 94.40%, indicated that **MTP5⊃HB-Cu** displayed excellent removal capacity toward CN^- in aqueous solution (Table 1). Meanwhile, the **MTP5⊃HB-Cu** could be extracted by dichloromethane and reused (Fig. S14 in Supporting information). Portable test kits were prepared for convenient detection of CN- (Fig. S16 in Supporting information). These results are of great significance to detect and remove extreme toxic CN^- in water.

In summary, we successfully constructed a supramolecular polymer gel **MTP5⊃HB**, which emitted bluish white AIE fluorescence and could ultrasensitively detect Cu^{2+} and Fe^{3+}. Meanwhile, the corresponding metallogel **MTP5⊃HB-Cu** could be used to continuously detect CN^- with high selectivity and ultrasensitivity. More importantly, the xerogel of **MTP5⊃HB-Cu** showed efficient removal ability for CN^- with 94.40% removal rate. Meanwhile, the portable test kit was also prepared for convenient and quick detection of CN^-.

Declaration of competing interest

The authors declare that they have no known competing financial interests or personal relationships that could have appeared to influence the work reported in this paper.

Acknowledgments

This work was supported by the National Natural Science Foundation of China (Nos. 21661028, 21662031, 21574104), and the Program for Changjiang Scholars and Innovative Research Team in University of Ministry of Education of China (No. IRT 15R56).

Appendix A. Supplementary data

Supplementary material related to this article can be found, in the online version, at doi:https://doi.org/10.1016/j.cclet.2019.09.046.

References

[1] L.L. Wang, J. Zheng, S. Yang, et al., ACS Appl. Mater. Interfaces 7 (2015) 19509–19515.
[2] Z.Z. Dong, C. Yang, K. Vellaisamy, et al., ACS Sens. 2 (2017) 1517–1522.
[3] N. Mergu, J.H. Moon, H. Kim, et al., Sens. Actuators B: Chem. 273 (2018) 143–152.
[4] Y. Shiraishi, M. Nakamura, N. Hayashi, et al., Anal. Chem. 88 (2016) 6805–6811.
[5] E. Jaszczak, Z. Polkowska, S. Narkowicz, et al., Environ. Sci. Pollut. Res. 24 (2017) 15929–15948.
[6] C.F. Chow, P.Y. Ho, W.L. Wong, et al., Chem. -Eur. J. 21 (2015) 12984–12990.
[7] C.H. Zong, L.R. Zheng, W.H. He, et al., Anal. Chem. 86 (2014) 1687–1692.
[8] P. Eskandari, M. Farhadian, A.R.S. Nazar, et al., Ind. Eng. Chem. Res. 58 (2019) 2099–2112.
[9] L. Brunsveld, B.J.B. Folmer, E.W. Meijer, et al., Chem. Rev. 101 (2001) 4071–4098.
[10] H. Li, Y. Yang, F.F. Xu, et al., Chem. Commun. 55 (2019) 271–285.
[11] T. Xiao, L. Wang, Chin. Chem. Lett. 29 (2018) 1172–1182.
[12] C.W. Zhang, B. Ou, S.T. Jiang, et al., Polym. Chem. 9 (2018) 2021–2030.
[13] Z.C. Gao, Y.F. Han, S.H. Chen, et al., ACS Macro Lett. 6 (2017) 541–545.
[14] Q. Lin, G.F. Gong, Y.Q. Fan, et al., Chem. Commun. 55 (2019) 3247–3250.
[15] H.G. Fu, Y. Chen, Y. Liu, ACS Appl. Mater. Interfaces 11 (2019) 16117–16122.
[16] T. Ogoshi, S. Kanai, S. Fujinami, et al., J. Am. Chem. Soc. 130 (2008) 5022–5023.
[17] C.J. Li, Chem. Commun. 50 (2014) 12420–12433.
[18] T. Ogoshi, T. Kakuta, T. Yamagishi, Angew. Chem. Int. Ed. 58 (2019) 2197–2206.
[19] P. Li, Y. Cheng, Y. Liu, Chin. Chem. Lett. 30 (2019) 1190–1197.
[20] S. Sun, J.B. Shi, Y.P. Dong, et al., Chin. Chem. Lett. 24 (2013) 987–992.
[21] Y. Wang, M.Z. Lv, N. Song, et al., Macromolecules 50 (2017) 5759–5766.
[22] Z.Y. Li, Y.Y. Zhang, C.W. Zhang, et al., J. Am. Chem. Soc. 136 (2014) 8577–8589.
[23] T. Xiao, L. Zhou, L. Xu, et al., Chin. Chem. Lett. 30 (2019) 271–276.
[24] J. Chen, Y. Wang, C. Wang, et al., Chem. Commun. 55 (2019) 6817–6826.
[25] S. Sun, D. Lu, Q. Huang, et al., J. Colloid. Interf. Sci. 533 (2019) 42–46.
[26] J.D. Luo, Z.L. Xie, J.W.Y. Lam, et al., Chem. Commun. 18 (2001) 1740–1741.
[27] Y.N. Hong, J.W.Y. Lam, B.Z. Tang, Chem. Soc. Rev. 40 (2011) 5361–5388.
[28] D. Ding, K. Li, B. Liu, et al., Acc. Chem. Res. 46 (2013) 2441–2453.
[29] D.H. Dai, Z. Li, J. Yang, et al., J. Am. Chem. Soc. 141 (2019) 4756–4763.
[30] J. Huang, N. Sun, P.Y. Chen, et al., Chem. Commun. 50 (2014) 2136–2138.
[31] P. Wang, B.C. Liang, D.Y. Xia, Inorg. Chem. 58 (2019) 2252–2256.
[32] A. Pankajakshan, D. Kuznetsov, S. Mandal, Inorg. Chem. 58 (2019) 1377–1381.
[33] L.W. Ma, S. Wang, C.P. Li, et al., Chem. Commun. 54 (2018) 2405–2408.
[34] Y.M. Zhang, W. Zhu, W.J. Qu, et al., Chem. Commun. 54 (2018) 4549–4552.
[35] J. Mei, N.L.C. Leung, R.T.K. Kwok, et al., Chem. Rev. 115 (2015) 11718–11940.
[36] L.Q. Shangguan, H. Xing, J.H. Mondal, et al., Chem. Commun. 53 (2017) 889–892.
[37] S.L. Wang, Y.L. Wang, Z.X. Chen, et al., Chem. Commun. 51 (2015) 3434–3437.
[38] N. Malviya, M. Das, P. Mandal, et al., Soft Matter 13 (2017) 6243–6249.
[39] X.D. Chi, M. Xue, Y. Yao, et al., Org. Lett. 15 (2013) 4722–4725.
[40] S. Nagashima, T. Ozawa, Int. J. Environ. Anal. Chem. 10 (1980) 99–106.
[41] L.F. Zhang, J.S. Zhang, Z.F. Zheng, et al., Anal. Chem. 91 (2019) 8762–8766.